

Bayesian Particle Tracking of Traffic Flows

Nicholas Polson
Booth School of Business, University of Chicago
and
Vadim Sokolov
Argonne National Laboratory

November 8, 2018

ABSTRACT

We develop a Bayesian particle filter for tracking traffic flows that is capable of capturing nonlinearities and discontinuities present in flow dynamics. Our model includes a hidden state variable that captures sudden regime shifts between traffic free flow, breakdown and recovery. We develop an efficient particle learning algorithm for real time on-line inference of states and parameters. This requires a two step approach, first, resampling the current particles, with a mixture predictive distribution and second, propagation of states using the conditional posterior distribution. Particle learning of parameters follows from updating recursions for conditional sufficient statistics. To illustrate our methodology, we analyze measurements of daily traffic flow from the Illinois interstate I-55 highway system. We demonstrate how our filter can be used to infer the change of traffic flow regime on a highway road segment based on a measurement from freeway single-loop detectors. Finally, we conclude with directions for future research.

INTRODUCTION

Modeling traffic dynamics for a transportation network with highways, arterial roads and public transit is an important task for effectively managing traffic flow. A major goal is to provide traffic flow conditions on highways from field measurements fusing in-ground loop detectors or GPS probes. Traffic managers make decisions based on model forecasts to regulate ramp metering, apply speed harmonization, or change road pricing as congestion mitigation strategies. The general public uses model-based predictions for assessing departure times, and travel route choices, among other factors.

We propose a dynamic state-space model which incorporates a latent switching variable together with a traffic flow state variable to capture the non-linearities and discontinuities in traffic patterns. Our dynamic model allows for three traffic flow regimes: free flow, breakdown and recovery. A physical interpretation of the change in the flow regime is a traffic queue with congestion inside the queue and free flow outside. In addition to switching variable and traffic flow states, we track a state that measures the rate of degradation or recovery. The challenge is to filter traffic flow measurements which are sparse, from both fixed and moving sensors which are located at a small number of locations at any given point in time. Statistical inference is further complicated by noisy non-Gaussian observations; for example, Rasschaert (1) show that the data generating distribution for video cameras is a mixture of Poissons.

In order to achieve real-time sequential inference, we develop an efficient particle filter and learning algorithm. This allows us to track the speed of traffic flow together with the latent states that describe regime switches, and the rate of degradation (recovery). To illustrate our methodology, we model a data from a network of in-ground loop detectors on Chicago's Interstate I-55 with measurements on speed, counts and occupancy of traffic flow. The sequential nature of particle filtering makes frequent updating feasible, and therefore, our method provides an alternative to Markov Chain Monte Carlo (MCMC) simulation methods. The computational cost of the latter grows linearly with the number of observations. We build on particle filters for traffic flow problems (see Mihaylova et al. (2)) who use the evolution dynamics as a proposal distribution before re-sampling, the so-called bootstrap or sampling/importance resampling (SIR) filter. We improve the filtering efficiency by developing a Rao-Blackwellized which is also flexible enough to incorporate particle learning.

Our approach builds upon existing statistical methods in a number of ways. Tebaldi and West (3) infer network route flows and Westgate et al. (4) develop MCMC methods to estimate travel time reliability for ambulances using noisy GPS for both path travel time and individual road segment travel time distributions. Anacleto et al. (5) propose a dynamic Bayesian network to model external intervention techniques to accommodate situations with suddenly changing traffic variables. Another class of probabilistic methods rely on using image processing techniques for traffic estimation, for example in Kamijo et al. (6) authors developed an algorithm that is based on Markov random field that allows analyzing images from intersections to detect flows and accidents.

Small changes in consecutive speed measurements can be explained by sensor noise but significant changes require estimation of probability of a flow regime switch, which is represented by a discontinuity in traffic flow speed. Previous work on estimating traffic flows use extensions of the Kalman filter and relies heavily on Gaussianity assumptions, see Gazis and Knapp, Schreiter et al., Wang and Papageorgiou, Work et al. (7, 8, 9, 10). Recently, Blandin et al., Polson and Sokolov (11, 12) showed that dynamic properties of traffic flow such as dis-

continuities (or shock waves), lead to forecast distributions that are mixtures. Our non-Gaussian state-space model will explicitly capture such a behavior.

Our approach builds on the current literature in a number of ways:

- Provides a hierarchical model rather than a conservation law based model. Our approach avoids boundary condition estimation
- A predictive likelihood particle filter provides an efficient estimation strategy. Our filter is less sensitive to measurement outliers and less prone to particle degeneracy
- Tracks traffic flow variables, such as traffic flow speed together with additional latent variables for regime switching and a degeneracy (recovery) rate.

One class of previously considered problems involves estimating (i) turn counts on urban controlled intersections [Lan and Davis, Ghods and Fu (13, 14)], (ii) flows or travel times on network routes [Kwong et al., Wu et al., Rahmani et al., Nantes et al., Fowe and Chan, Dell’Orco et al. (15, 16, 17, 18, 19, 20)], (iii) travel times and densities on an individual road segment [Coifman and Kim, Zheng and Van Zuylen, Zhan et al., Seo and Kusakabe, Seo et al., Bachmann et al. (21, 22, 23, 24, 25, 26)], and (iv) queue position on highways or arterial roads [Vigos et al., Ban et al., Zhan et al., Lee et al. (27, 28, 29, 30)]. There are several types of algorithms, which can be categorized into the following groups (i) time series analysis, (ii) machine or deep learning, and (iii) model-based analysis in a form of state-space models. We tackle the latter, which requires a particle filtering algorithm to perform inference.

A machine-learning algorithm was provided by Sun et al. (31), where authors proposed a Bayes network algorithm for forecasting traffic flow. The idea is to derive the conditional probability of a traffic state on a given road, given states on topological neighbors on a road network. The resulting joint probability distribution is a mixture of Gaussians. Bayes networks for estimating travel times were suggested earlier by Horvitz et al. (32). This approach eventually became a commercial product that led to the start of Inrix, a traffic data company. Wu et al. (33) provides a machine-learning method based on a support vector regression (SVR) to forecast travel-times and Quek et al. (34) use a fuzzy neural-network approach to address the issue of traffic data generating processes being non-linear and used fuzzy logic to improve the interoperability of their model. On the contrary, Rice and van Zwet (35), argue that there is a linear relation between the future travel times and currently estimated conditions. They demonstrate that a regression model with time varying coefficients is capable of designing a travel time prediction scheme. Another class of forecasting models relies on classical time series modeling. For example, Tan et al. (36) studied two classes of time series methods, auto-regressive moving average (ARIMA) and exponential smoothing (ES). The forecasts generated by ARIMA and ES models are used as inputs to neural networks, which aggregates those into a single forecast. Van Der Voort et al. (37) also proposed combing an ARIMA model with a machine learning method, the Kohonen self-organizing map, which was used as an initial classifier. Van Lint (38) addresses a parameter estimation problem of real-time learning that can improve the quality of forecasts via an extended Kalman filter for incorporating data in real-time into a parameter learning process. Ban et al. (39) proposes a method for estimating queue lengths at controlled intersections, based on the travel time data measured by GPS probes. The method relies on detecting discontinuities and changes of slopes in travel time data. Another data-mining based approach for queue

state estimation was proposed in Ramezani and Geroliminis (40), who combined the traffic flow shockwave analysis with data mining techniques.

Cheng et al. (41) proposes a threshold-based critical point extraction algorithm, with a goal to reduce the communication cost in the future real-time probe data collection application. A probabilistic approach, proposed in Hoffleitner et al. (42) uses a learning algorithm to infer the density of vehicles on arterial roads. A heuristic filter that allows combining data from multiple types of sensors with different spatial and temporal resolutions was proposed in Van Lint and Hoogendoorn (43).

Our main contribution is an algorithm for quick detection of the break-downs and recoveries in the traffic flow regimes. In many cases, we can detect the breakdown new measurement arrives. We contrast the performance of our filter with some other approaches in the “Numerical Experiments” subsection.

BAYESIAN MODELING OF TRAFFIC FLOW SPEED

Traffic flow speed data often relies on sparse and noisy measurements. Sparseness occurs due to a fixed grid of sensor or a dynamically changing data source such as GPS probes. Our state-space model is designed to be applicable in both scenarios. There are discontinuities in the traffic flow dynamics which need to be accounted for. We build a Dynamic Model [West and Harrison, Carlin et al. (44, 45)] for the traffic state during three regimes: free flow, breakdown and recovery.

To illustrate our methodology, we use data from a sensor on I-55 with id *N-6041*. The sensor is located eight miles from the Chicago downtown on I-55 north bound (near Cicero Ave), which is part of a route used by many morning commuters to travel from southwest suburbs to the city. As shown on Figure 1, the sensor is located 840 meters downstream of an off-ramp and 970 meters upstream from an on-ramp.

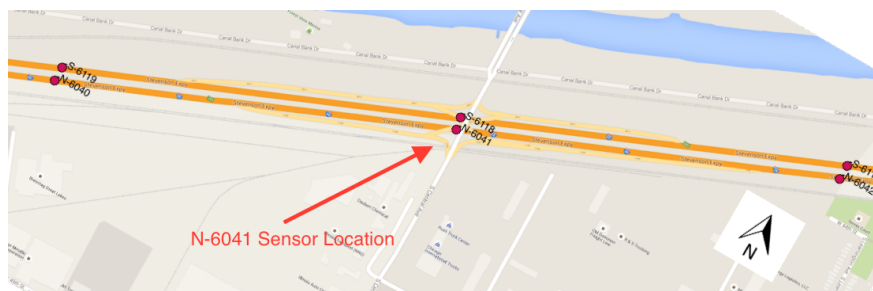


FIGURE 1 Location of the N-6041 sensor and the geometry of the road segment.

Figure 2 illustrates a typical day traffic flow pattern on Chicago’s I-55 highway where sudden breakdowns are followed by a recovery to free flow regime. This traffic pattern is recurrent and similar to one observed on other work days. We can see a breakdown in traffic flow speed during the morning peak (region 2) period followed by speed recovery (region 3). The free flow regimes (regions 1,4, and 5 on the plot) are usually of little interest to traffic managers. This data motivates our choice of the statistical model developed. The goal is to build a model that is capable of capturing the sudden regime changes, such as free flow to congestion at the beginning

of the morning rush hour (regions 1 and 2) or change in speed to the recovery regime at the end of the rush hour (regions 2 and 3).

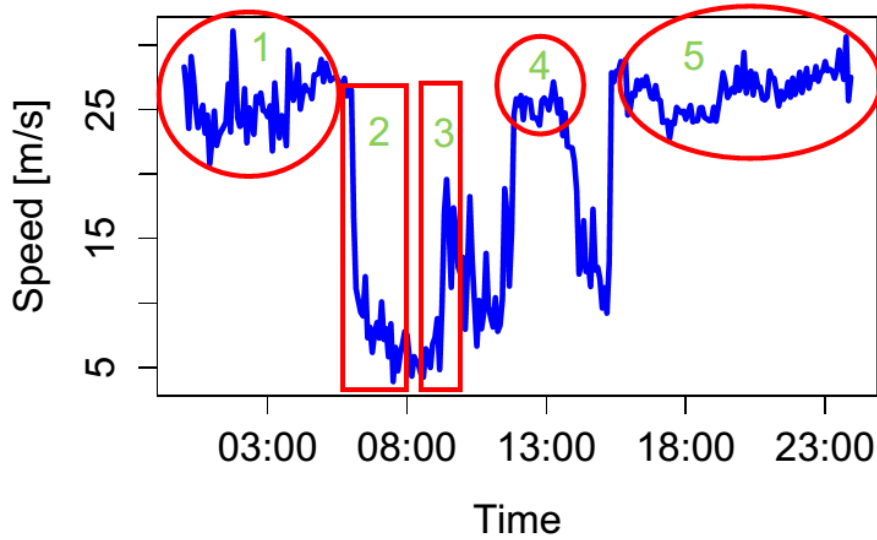


FIGURE 2 Example of one day speed profile on May 14, 2009 (Thursday). This plot illustrates the speed profile for a segment of interstate highway I-55. Different flow regime regions were identified and labeled by the authors.

A key modeling feature is the inclusion of a switching state variable $\alpha_{t+1} \in \{-1, 0, 1\}$ to identify different flow regimes. Trends during the break-down periods and recovery periods can then be modeled using the first order polynomial component.

Specifically, given a discretization from t to $t + \Delta t$, we use a state-space model of the form

$$\text{Observation: } y_{t+1} = Hx_{t+1} + \gamma^T z_{t+1} + v_{\alpha_{t+1}}, \quad v_{\alpha_{t+1}} \sim N(0, V_{\alpha_{t+1}}) \quad (1)$$

$$\text{Evolution: } x_{t+1} = G_{\alpha_{t+1}} x_t + (I - G_{\alpha_{t+1}})\mu + w_{t+1}, \quad w_{t+1} \sim N(0, W_{\alpha_{t+1}}) \quad (2)$$

$$\text{Switching Evolution: } \alpha_{t+1} \sim p(\alpha_{t+1} | \alpha_t, Z_t) \quad (3)$$

where evolution gain matrix is

$$G_{\alpha_{t+1}} = \begin{pmatrix} F_{\alpha_{t+1}} & \alpha_{t+1} \\ 0 & 1 \end{pmatrix}, \quad \text{and } \mu = \begin{pmatrix} v_f \\ 0 \end{pmatrix}$$

Our hidden state variable $x_t = (\theta_t, \beta_t)^T$, where θ_t is traffic flow speed and β_t is rate of change. We model the recovery and degradation in speed using an additive component $\alpha_t \beta_t$. We also model β_t using a random walk model. Measurements are then given by $y_t = (\text{speed}, \text{count}, \text{density})_t$, and we incorporate a switching variable with three states $\alpha_t \in \{\text{breakdown}, \text{free flow}, \text{recovery}\}_t$.

The observation matrix H , which could be time varying, allows for partial observation of the state vector x_t . The parameter v_f the free flow speed on the road segment. We allow for the possibility of regressors, z_{t+1} , in the observation equation which effect the sensor measurement

model, γ are regressors parameters. The switching coefficient F_{α_t} defines weather the process is mean-reverting or not. We define it by

$$F_{\alpha_t} = \begin{cases} 1, & \alpha_t \in \{1, -1\} \\ F_0, & \alpha_t = 0. \end{cases},$$

where $F_0 < 1$ is the rate of mean-reversion during a free flow regime. The dynamics $p(\alpha_{t+1}|\alpha_t, Z_t)$ of the switching evolution depends on the set of variables Z_t , that explain regime shifts. Several approaches to model switching process $p(\alpha_{t+1}|\alpha_t, Z_t)$ and choosing Z_t are described in the next sub-section.

The main task of our approach is to detect the start of breakdown and recovery as soon as possible. The causes of breakdown or recovery might be different. For example a breakdown might be caused by a recurrent demand that increases capacity or non-recurrent conditions, such as weather or traffic accidents. Characteristic change in the traffic flow speed would be the same in either situation and thus our model is agnostic to the cause of the start or end of a congestion period.

Modeling $p(\alpha_{t+1}|\alpha_t, Z_t)$

The discrete state $\alpha_{t+1} \in \{-1, 0, 1\}$ models breakdown ($\alpha = -1$), free flow ($\alpha = 0$), and recovery ($\alpha = 1$) regimes of a traffic system. We need to specify a transition kernel for the evolution of this state given a set of exogenous predictor variables, denoted by Z_t , and current state α_t . Given Z_t , the set of probabilities, $p(\alpha_{t+1}|\alpha_t, Z_t)$, will then form a 3×3 matrix which will be combined with the evolution of the hidden state vector x_t .

Figure 4 shows that break downs happen more or less the same time during morning or evening peak periods on a work day. Therefore, it is natural to introduce an exogenous variable $Z_t = (\text{period}, \text{day of week})$, $\text{period} \in \{1, 2, 3\}$ where the three periods correspond to morning, evening peak period and the rest of the day. Incorporating additional considerations beyond a period of the day and day of the week, such as weather, month, and special event leads to

$$Z_t = (\text{day of week}, \text{month}, \text{weather}, \text{month}, \text{event}, \text{accident})_t.$$

One way to build such a model is to identify 3×3 transition matrix $p(\alpha_{t+1}|\alpha_t, Z_t)$ for each combination of the parameters in Z_t based on the historic observations.

Figure 3(a) shows the average speed for a fixed location on the network for the April 4 - March 3 period in 2009, weekend days identified by blue dots. We see that the average speed on weekend is very close to free flow speed, roughly 63 mi/h, which means there is no congestion on those days. On the other hand average speed on a work day is significantly lower as a result if congestion during rush hour. We also can see an unusual average speed on April 10 of 2009 (seventh observation). It was Good Friday. Thus, far less traffic was observed compared to a typical Friday.

Figure 3(b) shows a scatter plot of measured traffic flow speed for all non-holiday Wednesdays in 2009. The measurements are taken every five minutes. We can see that congestion starts roughly at the same time at around six in the morning and lasts roughly for three hours. The breakdown in the evening happens less frequently.

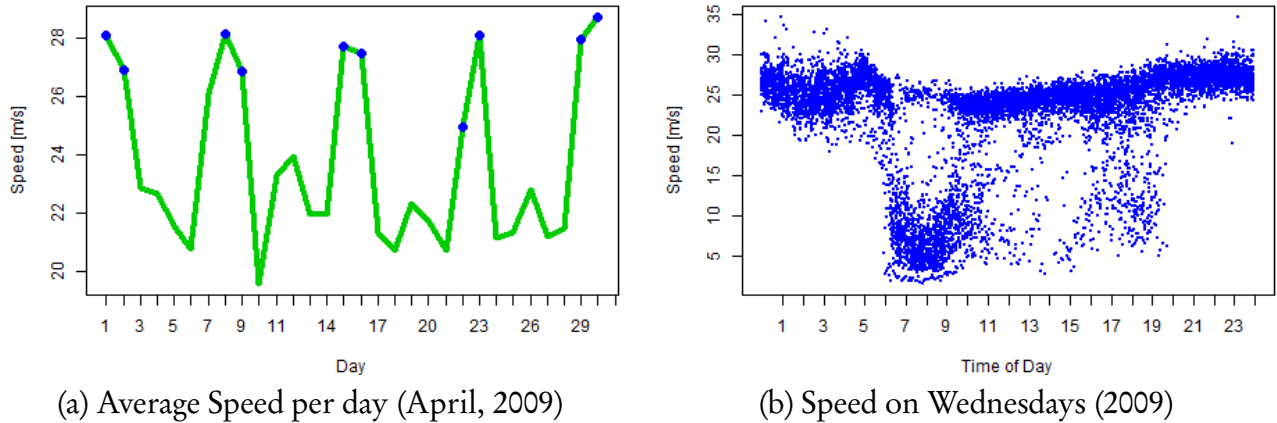


FIGURE 3 Recurrent traffic flows. The left panel (a) shows average speed as measured by the sensor N-6041 for each day during the April 4 - March 3 of 2009 time period. Weekends are marked by blue dot. The right panel (b) shows raw speed measurements from the sensor N-6041 for each five minute interval of every Wednesday in 2009.

Another effect to be modeled is traffic congestion that is a recurrent event, and is similar from one week to another. Figure 4 shows the recurrent traffic conditions grouped by the day of the week. This observation can be used to choose Z_t . In particular, an approach based on non-parametric regression that uses historical traffic flow data. For example, Smith et al. (46) and Chiou et al. (47) showed that the last three measured speed values, perform very well for predicting traffic flows. In this case we can write Z_t as

$$Z_t = (\alpha_t, \hat{x}_t, \hat{x}_{t-1}, \hat{x}_{t-2}, \text{time of day})^T,$$

where \hat{x}_t is the filtered value of state vector x_t . Then the transition dynamics $p(\alpha_{t+1} | \alpha_t, Z_t)$ is generated by computing a weighted average of those points from historic database that fall within a neighborhood of Z_t . To calculate the neighborhood, we calculate distance between Z_t and each of the point from the data base, and then choose k points with smallest distance. The weights are proportional to the distance.

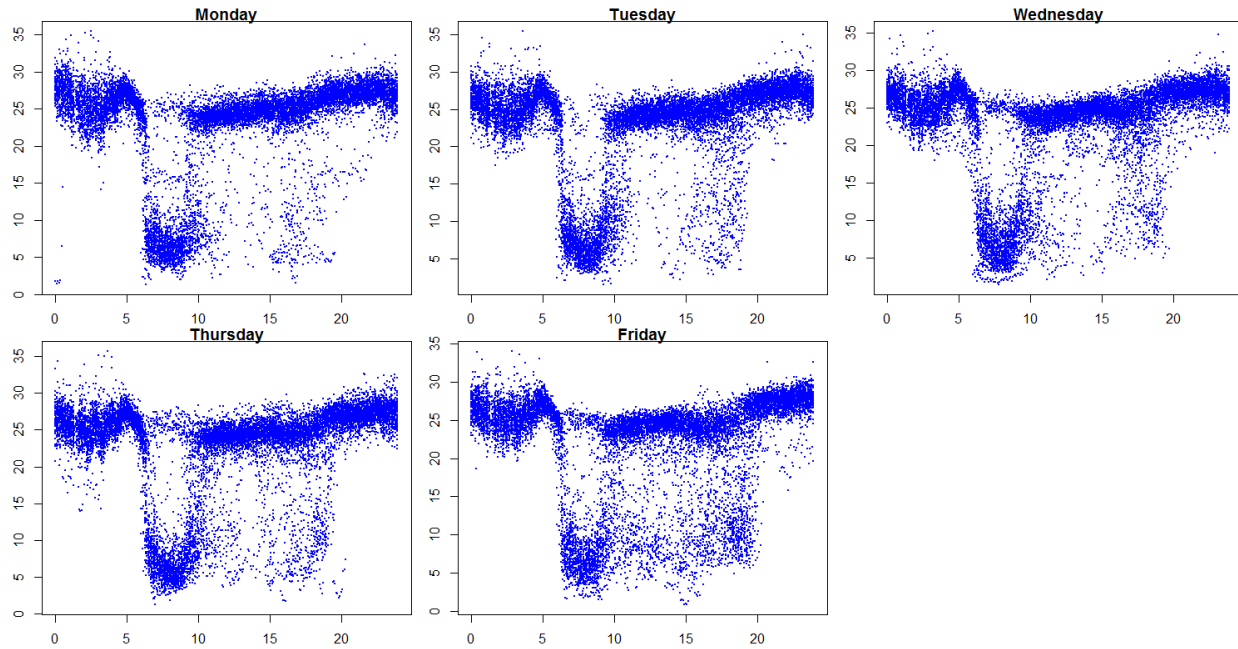


FIGURE 4 Daily Traffic Patterns, measured in 2009. Each plot shows raw speed measurements averaged over five minute intervals from the sensor N-6041 for a given day of the week, with holidays and days with erroneous measurements removed from data.

TRACKING TRAFFIC FLOWS DURING SPECIAL AND WEATHER EVENTS

Our model is flexible in the sense that we can handle special events or severe weather conditions that can upset a typical traffic patterns. To show the empirical effect of snowy weather, Figure 5 compares the expected travel time (red line), which is calculated based on historical data for the last 150 days, with the travel time on a snow day (green line), for December 11, 2013. There were 1.8 inches of snow on this day, with snow starting at midnight and continuing till noon. There were no traffic accidents on this road segment on this day. As we can see, even a light snow in a region, where drivers are used to driving during snow days can cause major delays. The yellow region is the 70% confidence interval based on historical data.

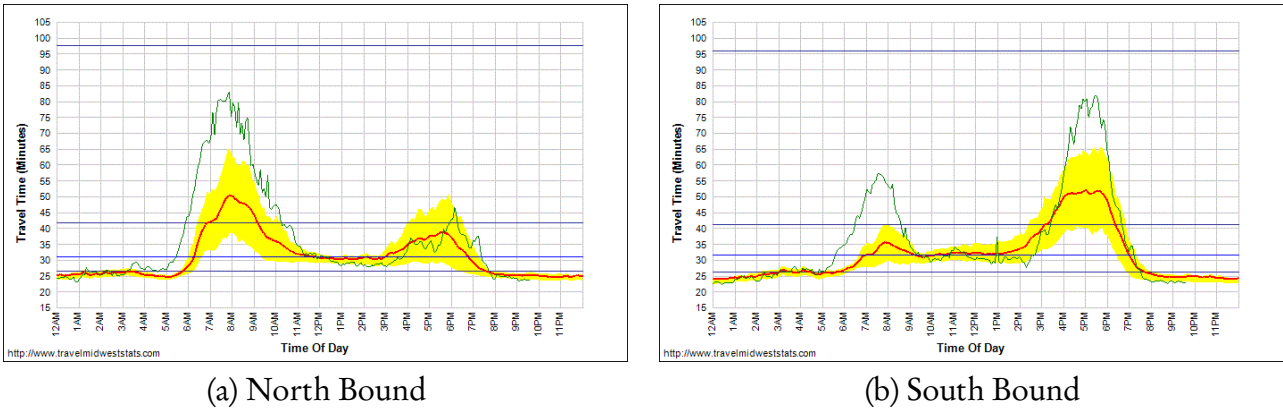
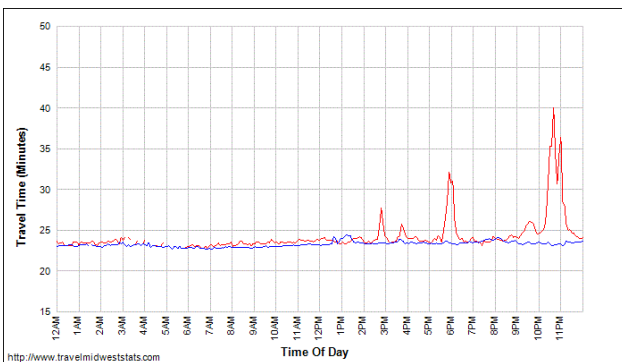
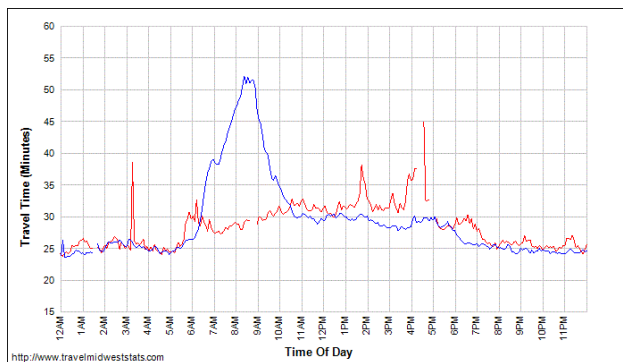


FIGURE 5 Impact of light snow on travel times on I-55 near Chicago on December 11, 2013. Both plots show travel time on a 27 mile stretch of highway I-55 between I-355 and I-94 in both north and south directions. The north bound direction is from southwest suburbs to the city. The red line is a travel time averaged over previous 150 days, the yellow area show 70% confidence interval for the data and green line is the travel time on the day of the event. Source: www.travelmidweststats.com

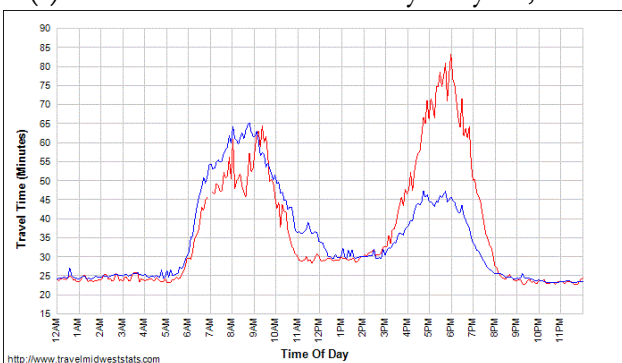
Special events is another potential cause of unusual traffic conditions. Figure 6 shows impacts of special events on travel times on interstate I-55 north bound (towards the city). The weekday football game, which takes place at Solder Field stadium in Chicago downtown, combined with typical commute traffic has a very significant impact on travel times. Weekend special events have a relatively minor negative impact. On the other hand, the NATO summit that was held in Chicago's McCormick Place located slightly south of downtown on Monday, had positive impact on travel times. This can be explained away by regular commuters, who knew about the event, changing their departure times, using commuter rail or simply working from home on this day.



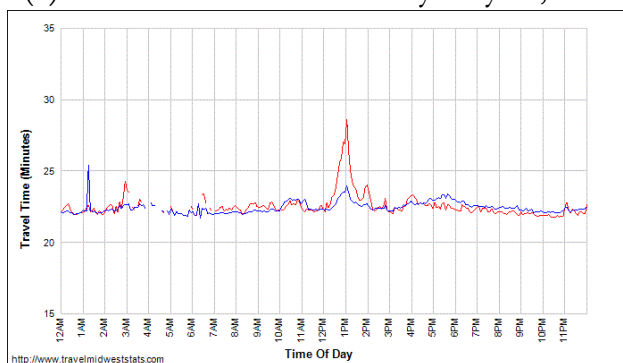
(a) NATO Summit on Sunday May 20, 2012



(b) NATO Summit on Monday May 21, 2012



(c) New York Giants at Chicago Bears on Thursday October 10, 2013



(d) Baltimore Ravens at Chicago Bears on Sunday November 10, 2013

FIGURE 6 Impact of special events on I-55 north bound travel times. All plots show travel time on a 27 mile stretch of highway I-55 between I-355 and I-94 in both north (towards the city) and south directions. All plots compare travel times on the day of the special event (red line) with the travel time on the same day of the week averaged over the previous 150 days (blue line). www.travelmidweststats.com

BUILDING A PARTICLE FILTER

Given our state-space model, the goal is to provide an on-line algorithm, for finding, in an on-line fashion, the set of joint filtered posterior distributions $p(x_t, \alpha_t | y_{1:t})$ using a two-step procedure for both x_t, α_t , the traffic flow state, and switching variable at each time point. The advantage of particle filtering is that we simply re-sample from the predictive distribution of the current posterior and then propagate, to the next set of particles, to generate the approximation to the conditional posterior update. Appendix A provides a review of particle filtering and learning methods.

From a probabilistic viewpoint, we can re-write equations (1) - (2) as a hierarchical model

$$(y_{t+1} | x_{t+1}) \sim N(Hx_{t+1} + \gamma^T z_{t+1}, V_{\alpha_{t+1}}) \quad (4)$$

$$(x_{t+1} | x_t, \alpha_{t+1}) \sim N(G_{\alpha_{t+1}} x_t + (I - G_{\alpha_{t+1}})\mu, W_{\alpha_{t+1}}). \quad (5)$$

Now, suppose that we are currently at time t . We assume a particle approximation for

the joint posterior of (x_t, α_t) is of the form

$$p^N(x_t, \alpha_t | y^t) = \sum_{i=1}^N w_t^{(i)} \phi(x_t, m_t^{(i)}, C_t^{(i)}) \delta_{\alpha_t^{(i)}}(\alpha_t)$$

where $y^t = (y_1, \dots, y_t)$ and $\delta_{\alpha}(\cdot)$ is a Dirac measure and $w_t^{(i)}$ is a set of particle weights, which we will provide recursive updates for. We denote the Kalman moments by $s_t = (m_t, C_t)$ which form a set of conditional sufficient statistics for the state. We describe the recursions later. Here $\phi(x, \mu, C)$ denotes a normal density with mean μ and covariance C

$$\phi(x, \mu, C) = \frac{1}{(2\pi)^{\frac{k}{2}} |C|^{\frac{1}{2}}} \exp\left(-\frac{1}{2}(x - \mu)^T C^{-1}(x - \mu)\right).$$

To assimilate the next measurement, we need to find an updated posterior for (x_{t+1}, α_{t+1}) , with approximate weights $w_{t+1}^{(i)}$ and particles (x_{t+1}, α_{t+1}) of the form

$$p^N(x_{t+1}, \alpha_{t+1} | y^{t+1}) = \sum_{i=1}^N w_{t+1}^{(i)} \phi(x_{t+1}, m_{t+1}^{(i)}, C_{t+1}^{(i)}) \delta_{\alpha_{t+1}^{(i)}}(\alpha_{t+1}),$$

Our weights will be updated using the predictive likelihood, $p(y_{t+1} | s_t^{(i)})$, which are re-normalized. We aim to provide a posterior with the same number of particles N with mixture weights of the form

$$w_{t+1}^{(i)} = \frac{w_t^{(i)} p(y_{t+1} | (\alpha_t, s_t)^{(i)})}{\sum_{i=1}^N w_t^{(i)} p(y_{t+1} | (\alpha_t, s_t)^{(i)})}.$$

Recursive Updating

At time zero, we set an initial state distribution $p(x_0 | \alpha_0)$ as follows

$$p(x_0 | \alpha_0) = \sum_{i=1}^N w_{\alpha_0}^{(i)} \phi(x_0, \mu_{\alpha_0}^{(i)}, C_{\alpha_0}^{(i)})$$

We take $p(\alpha_0 = s) = 1/3$, $s \in \{-1, 0, 1\}$.

Conditional on the hidden switching state α_t , the Kalman filter recursions, imply that filtered posterior distribution at time t is also mixture multivariate normal, i.e

$$p^N(x_t | \alpha_{1:t}, y_{1:t}) = \sum_{i=1}^N w_t^{(i)} \phi(x_t, m_t^{(i)}, C_t^{(i)})$$

where $(m_t, C_t)^{(i)}$ are functions of the whole path $\alpha_{1:t}, y_{1:t}$.

The goal is to find the next filtered posterior $p(x_{t+1} | y_{1:t+1})$, which is obtained from the marginal of the joint posterior $p(x_{t+1}, \alpha_{t+1} | y_{1:t+1})$.

Given, that $x_t \sim N(m_t, C_t)$, from evolution equation (5), it follows that

$$p(x_{t+1} | \alpha_{t+1}, s_t) = \phi(x_{t+1}, G_{\alpha_{t+1}} m_t + (I - G_{\alpha_{t+1}}) \mu, G_{\alpha_{t+1}} C_t G_{\alpha_{t+1}}^T + W_{\alpha_{t+1}})$$

To implement this algorithm, first compute the predictive likelihood of the next observation y_{t+1} given α_{t+1}, s_t , where $s_t = (m_t, C_t)$ is the sufficient statistics. This can be done by marginalizing out x_{t+1} from measurement equation (4). We obtain a marginal predictive distribution

$$\begin{aligned} p(y_{t+1}|\alpha_{t+1}, s_t) &= \int p(y_{t+1}|\alpha_{t+1}, x_{t+1})p(x_{t+1}|\alpha_{t+1}, s_t)dx_{t+1} \\ &= \int \phi(y_{t+1}, Hx_{t+1} + \gamma^T z_{t+1}, V_{\alpha_{t+1}}) \\ &\quad \phi(x_{t+1}, G_{\alpha_{t+1}} m_t + (I - G_{\alpha_{t+1}})\mu, G_{\alpha_{t+1}} C_t G_{\alpha_{t+1}}^T + W_{\alpha_{t+1}})dx_{t+1} \\ &= \phi(y_{t+1}, \mu_{t+1}^y, V_{t+1}^p). \end{aligned}$$

where $\mu_{t+1}^y = H(G_{\alpha_{t+1}} m_t + (I - G_{\alpha_{t+1}})\mu) + \gamma^T z_{t+1}$, $V_{t+1}^p = V_{\alpha_{t+1}} + H^T (G_{\alpha_{t+1}} C_t G_{\alpha_{t+1}}^T + W_{\alpha_{t+1}}) H$ and $V_{\alpha_{t+1}}$ and $W_{\alpha_{t+1}}$ are given variance-covariance matrices.

We can further marginalize out α_{t+1} using the transition kernel $p(\alpha_{t+1}|\alpha_t, Z_t)$. This leads to 3-component mixture predictive model of the form

$$p(y_{t+1}|x_t, \alpha_t) = \sum_{\alpha_{t+1} \in \{0, 1, -1\}} \phi(y_{t+1}, \mu_{t+1}^y, V_{t+1}^p) p(\alpha_{t+1}|\alpha_t, Z_t)$$

Our model, therefore allows for heavy-tails and non-Gaussianity in the traffic flow evolution. We now show how this can be used to implement a particle filter and learning algorithm and track the filtered posterior distributions of the hidden state $p(x_t|y_{1:t})$ over time as new data y_{t+1} arrives.

Given (α_{t+1}, y_{t+1}) , we need to update $s_t = (\mu_t, C_t)^T$, where we suppress the index i for clarity.

These updates are given by Kalman recursion operator, \mathcal{K} , which is given by

$$\begin{aligned} \mu_t^f &= G_{\alpha_{t+1}} \mu_t + (I - G_{\alpha_{t+1}})\mu, & C_t^f &= G_{\alpha_{t+1}} C_t G_{\alpha_{t+1}}^T + W_{\alpha_{t+1}} \\ \mu_t &= \mu_t^f + K_t(y_t - H\mu_t^f), & C_t &= (I - K_t H_t) C_t^f \end{aligned}$$

with Kalman gain matrix

$$K_t = C_t^f H^T (H C_t^f H^T + V)^{-1}$$

Now we are in a position to find the predictive density in equation (6), namely $p(y_{t+1}|\alpha_t, s_t)$, which is a 3-component mixture of Gaussians. This will lead to an efficient Rao-Blackwellised particle filter

Algorithm. Particle Filtering for traffic flows:

Step 1 (Draw) an index $k_t(i) \sim \text{Multi}(w_{t+1})$ -distribution with weights

$$w_{t+1}^{(i)} = p(y_{t+1}|s_t^{(i)}) / \sum_{i=1}^N p(y_{t+1}|s_t^{(i)}). \quad (6)$$

Step 2 (Propagate) switching state $\alpha_{t+1}^{(i)} \sim p(\alpha_{t+1} | \alpha_t^{k_t(i)})$

Step 3 (Propagate) sufficient statistics $s_t^{k_t(i)}$ using assimilated data and Kalman filter recursion

$$s_{t+1}^{(i)} = \mathcal{K}(s_t^{k_t(i)}, \alpha_{t+1}^{(i)}, y_{t+1}) \quad (7)$$

The weights are updated according to the following rule

$$w_{t+1}^{(i)} = \frac{w_t^{(i)} p(\alpha_{t+1} | \alpha_t^{(i)})}{\sum_{i=1}^N w_t^{(i)} p(\alpha_{t+1} | \alpha_t^{(i)})}$$

Finally, we draw new state vector x_{t+1} from its mixture multivariate normal distribution.

TRACKING TRAFFIC FLOW ON INTERSTATE I-55

Dataset Description

The data was provided by the Lake Michigan Interstate Gateway Alliance

(<http://www.travelmidwest.com/>) formally Gary-Chicago-Milwaukee Corridor (GCM). The data are measurements from the loop-detector sensors installed on interstate highways. A loop detector is a very simple presence sensor that senses when a vehicle is on top of it and generates an on/off signal. There are slightly more than 900 loop-detector sensors that cover a large portion of the Chicago metropolitan area. Every 5 minutes a report for each of the loop detector sensors is recorded. Our data contains averaged *speed*, *flow*, and *occupancy*. Flow is defined as the number of off-on switches. Occupancy is defined as percentage of time a point on a road segment was occupied by a vehicle, thus it varies between 0 (empty road) to 100 (complete stand still). We assume a constant vehicle length, and treat speed derived from a single loop-detector occupancy measurement as the true traffic flow speed.

Numerical Experiments

Consider a single road segment. We use measured data for a 24-hour period taken on a week day. The segment we consider is a part of highway I-55 north bound. This part of the highway is heavily congested during the morning rush hour, mostly due to commuters, who travel from the south-west suburbs to the central business district of Chicago. There were no special events on that day and the weather was clear, thus a very similar congestion pattern can be observed on any “usual” work day on this road segment. The measurements are made by a single loop detector. For this example we calculate the filtering distribution for the travel speed, flow regime, and rate of change variables on this segment. The time series of measured speeds is of length $N = 288$ (24×12).

The state $x_t = (\theta_t, \beta_t)^T \in \mathbb{R}^2$ is a true travel speed and associated trend coefficient. The parameters of the observation and evolution models are set to:

$$H = (1 \ 0), \quad V_{\alpha_t} = 4, \quad F_0 = 0.5, \quad W_{\alpha_t} = \begin{pmatrix} 1.9 & 0 \\ 0 & 4.5 \end{pmatrix},$$

Given that we did not have access to manufacturer’s specifications of the loop detectors, we use a value for the measurement error within the guidelines of the specification. The error for the evolution equation was chosen using maximum a posteriori mode estimation based on the data from the previous 30 days.

In our simulation study, we define a transition matrix P with equilibrium probabilities $\pi P = \pi$ that calibrate well to the three states in practice. Thus, we construct a Markov-switching process with the following probability transition matrix

$$P_{\alpha_t} = \begin{pmatrix} 0.6 & 0.3 & 0.1 \\ 0.15 & 0.7 & 0.15 \\ 0.3 & 0.1 & 0.6 \end{pmatrix},$$

where $\alpha_t \in \{breakdown, free\ flow, recovery\}$. The transition probabilities were fitted using a maximum a posteriori mode estimator. F_0 was fitted using data from times when traffic is stationary, and W_{α_t} was fitted using the data from both the stationary and non-stationary regimes.

Figure 7 shows the filtered speed and its quantiles, along with measured data. We see that the filtered state curve more-or-less follows the measurement curve. The evolution model proposed in this paper is very general and allows large changes in the speed state. Thus, the jittering behavior of measurement get mostly explained by statistical model and does not get filtered out.

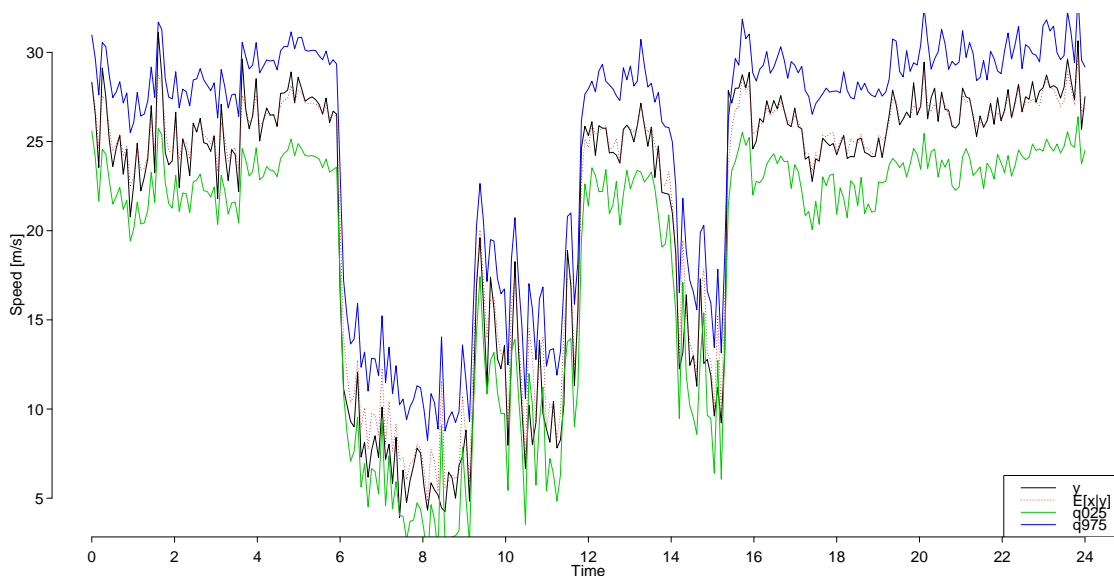


FIGURE 7 Filtered traffic speed given loop detector measurements.

Figure 8 shows the filtered probability of α for each of the values (0,1,-1). We can see that the algorithm accurately captures the changes in the flow regime, assigns high probability to free flow regime before the morning peak and the shifts probability to the breakdown regime.

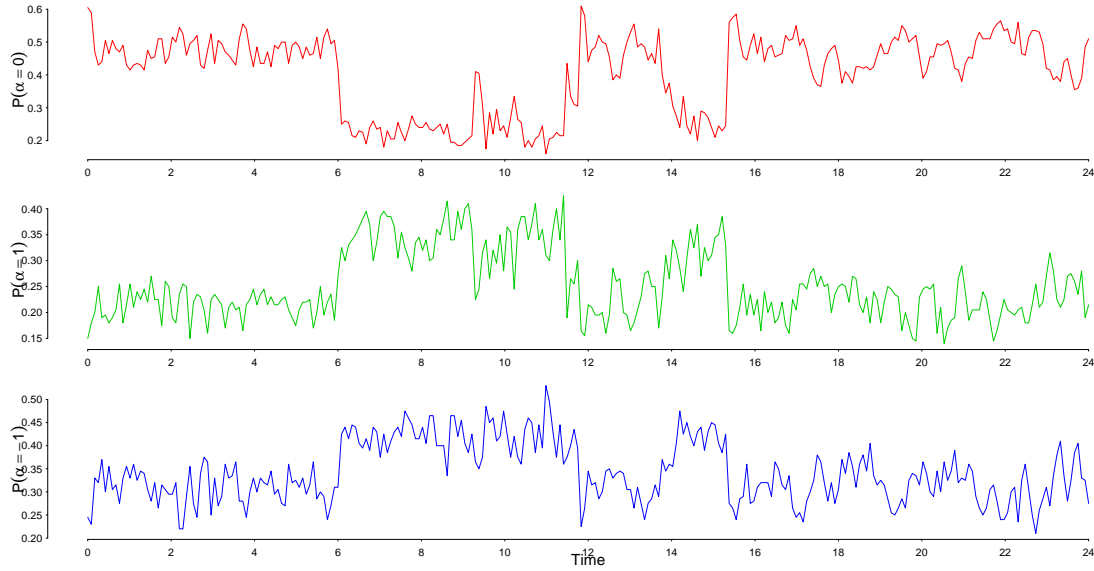


FIGURE 8 Filtered value of $P(\alpha = i)$, $i = 1, 2, 3$

Figure 9 shows the filtered values for rate of change of speed during recovery and breakdown regimes. The algorithm captures all of the changes in traffic flow change rates. The algorithm captures “fast” breakdown a little after 6am and “slow” breakdown at around 10am. It also captures, for example, the recovery between 2pm and 4pm.

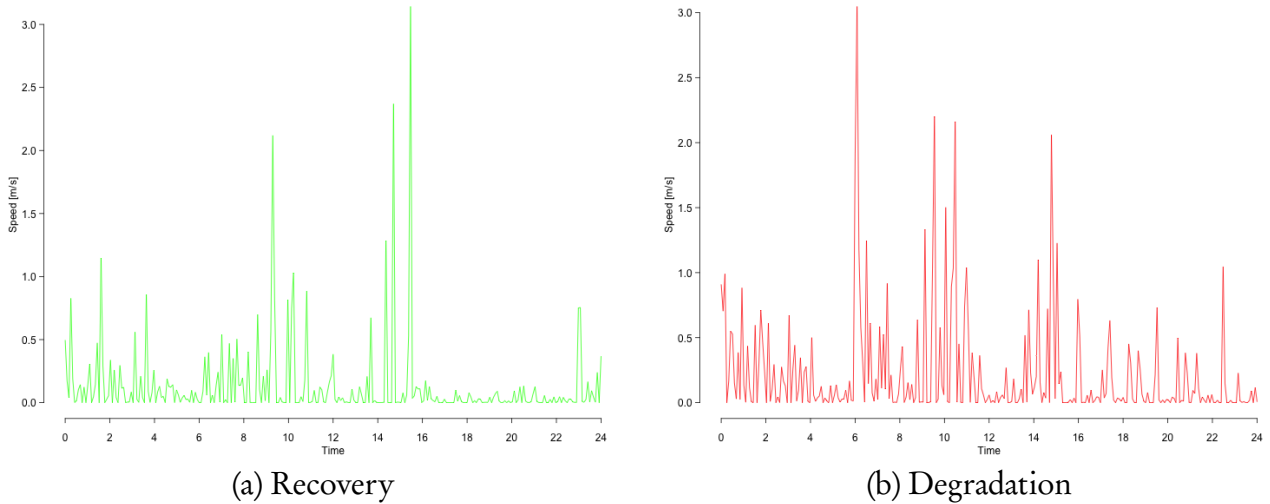


FIGURE 9 Rate of change of traffic flow

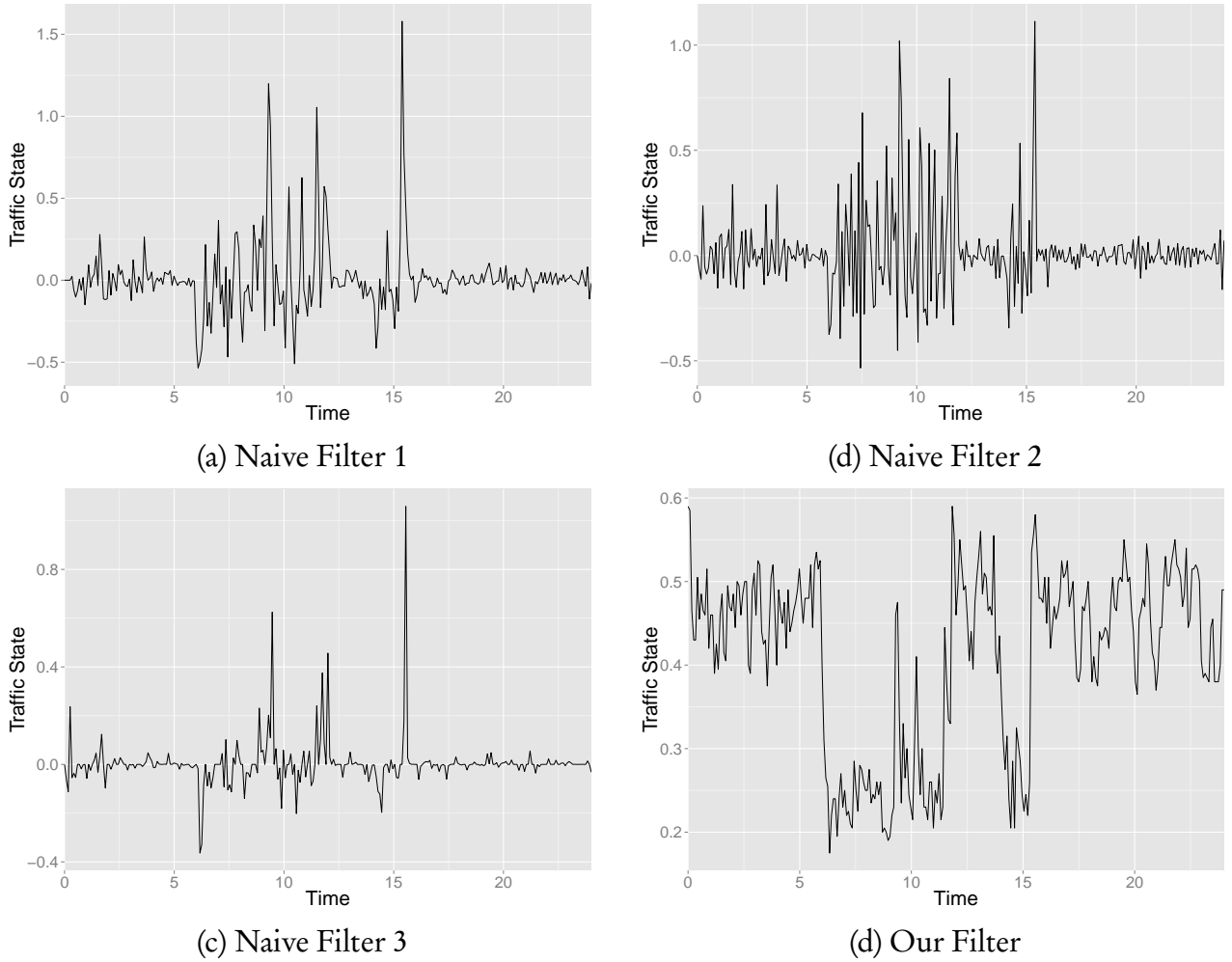


FIGURE 10 Comparison of filtered value of α with traffic states calculated using three other naïve filters

Naive filter 1 (mean filter): $\mu_i = \frac{1}{w} \sum_{j=i-w}^{i-1} y_j$, $y_i^f = \frac{y_i - \mu_i}{\mu_i}$

Naive filter 2 (simple smoothing): $y_i^f = \frac{y_i - y_{i-1}}{y_{i-1}}$

Naive filter 3 (quantile filter):

$$Y_i = \{y_{i-w}, \dots, y_{i-1}\}$$

$$Q_i := Pr(Y_i \leq y_i) = 0.5 \text{ (median)}$$

$$y_i^f = \frac{y_i - Q_i}{Q_i}$$

The results of numerical experiments illustrate the following features. The filtered speed plot follows the measurement plot, which is an expected result. We have chosen a well-behaving sensor for the study and there is no outliers in the measurements. The filtering algorithm properly identifies rate of change during break down and recovery regime. We can see that breakdown

happens faster. This is a well known fact, that it takes less time for a queue to build up than to dissipate. This difference in time can be explained by driver’s behavior and the fact that vehicles acceleration rate is lower than deceleration rate. However, the results for filtered probabilities of the switching variable α_t are less intuitive. Our filter properly identifies free flow regime in the morning, but then gets “slightly confused” during morning rush hour by assigning very close probabilities to recovery and breakdown regimes. We interpret this as saying that the Markov switching process model used to model $P(\alpha_t | \alpha_{t+1}, Z_t)$ is misspecified and need to be refined. This is a topic for our future research.

DISCUSSION

We propose a mixture state-space model together with a particle filter and learning for tracking the state of traffic flow and other hidden variables such as flow regime and rate of change in the traffic flow speed. The proposed method is flexible, in a sense that it does not require the state-space model to be Gaussian. Our approach does not rely on blind particle proposal for estimating the forecast distribution, but instead draws are taken from a smoothed distribution, which takes the measurement into consideration. Thus, our filter is fully adapted with exact samples from the filtering distribution are drawn. We used the sufficient statistics representation for state particles lead to a computationally efficient method. We formulate the traffic flow evolution equation as a hierarchical Bayesian model that is capable of capturing traffic flow discontinuities.

Although we have focused on representation of state-space dynamics using multi-process DLM, the same approach will work for the kinematic wave theory based approach. When the evolution equation is given by the classical macroscopic traffic flow model, namely Lighthill-Whitham-Richards (LWR) partial differential equation Lighthill and Whitham, Richards (48, 49). A Bayesian analysis of traffic flows using the LWR model is described in Polson and Sokolov (12). However, the analysis based on the LWR model requires an estimation of conditions for a road segment, which is not always available. The statistical model described in here has the flexibility to avoid assumptions on locations of sensors.

While we demonstrated the solution to the filtering problem in this paper, the fact that we provided a closed form solution to the filtering density and can do exact sampling from the filtering density allows us to use the same approach for particle learning and smoothing Carvalho et al. (50). It works by augmenting the particle space to $\{x_t, s_t\}$, where s_t is the sufficient statistic for the parameter space γ , i.e. $p(\gamma | x^t, y^t) = p(\gamma | \phi_t)$. In the DLM setting we can learn β , by removing the evolution equation for this parameter, rather than learning it directly from data, without relying on any model. Further research into predictive performance of such models is warranted.

PARTICLE FILTERING AND LEARNING METHODS

Particle filtering and learning methods are designed to provide state and parameter inference via the set of joint posterior filtering distribution obtained in an on-line fashion [Gordon et al. (51), Carpenter et al. (52), Pitt and Shephard (53), Storvik (54), Carvalho et al. (50)].

Let y_t denote the data, and θ_t the state variable, in our context use (x_t, α_t) . Let ϕ denote the unknown parameters. For the moment, we suppress the conditioning on the parameters ϕ . We will show how to update state variables and sufficient statistics for ϕ . First, we factorize the

joint posterior distribution of the data and state variables both ways as

$$\begin{aligned} p(y_{t+1}, \theta_{t+1} | \theta_t) &= p(y_{t+1} | \theta_{t+1}) p(\theta_{t+1} | \theta_t) \\ &= p(y_{t+1} | \theta_t) p(\theta_{t+1} | \theta_t, y_{t+1}) \end{aligned}$$

The goal is to obtain the new filtering distribution $p(\theta_{t+1} | y^{t+1})$ from the current $p(\theta_t | y^t)$. A particle representation of the previous filtering distribution is a random histogram of draws. It is denoted by $p^N(\theta_t | y^t) = 1/N \sum_{i=1}^N \delta_{\theta_t^{(i)}}$, where δ is a Dirac measure. As the number of particles increases $N \rightarrow \infty$ the law of large numbers guarantees that this distribution converges to the true filtered distribution $p(\theta_t | y^t)$.

In order to provide random draws of the next distribution, we first resample θ_t 's using the smoothing distribution

$$p(\theta_t | y^{t+1}) \propto p(y_{t+1} | \theta_t) p(\theta_t | y^t)$$

obtained by Bayes rule. Thus, we draw $\theta_t^{k(i)}$ by drawing the index $k(i)$ from a multinomial distribution with weights

$$w_t^{(i)} = \frac{p(y_{t+1} | \theta_t^{(i)})}{\sum_{j=1}^N p(y_{t+1} | \theta_t^{(j)})}.$$

We set $\theta_t^{(i)} = \theta_t^{k(i)}$ and “propagate” to the next time period $t + 1$ using the predictive

$$p(\theta_{t+1} | y_{1:t+1}) = \int p(\theta_{t+1} | \theta_t, y_{t+1}) p(\theta_t | y_{1:t+1}) d\theta_t.$$

Given a particle approximation $\{\theta^{(i)} : 1 \leq i \leq N\}$ to $p^N(\theta_t | y^t)$, we can use Bayes rule to write

$$\begin{aligned} p^N(\theta_{t+1} | y^{t+1}) &\propto \sum_{i=1}^N p(y_{t+1} | \theta_t^{(i)}) p(\theta_{t+1} | \theta_t^{(i)}, y_{t+1}) \\ &= \sum_{i=1}^N w_t^{(i)} p(\theta_{t+1} | \theta_t^{(i)}, y_{t+1}), \end{aligned}$$

where the particle weights are given by

$$w_t^{(i)} = \frac{p(y_{t+1} | \theta_t^{(i)})}{\sum_{i=1}^N p(y_{t+1} | \theta_t^{(i)})}.$$

This mixture distribution representation leads to a simple simulation approach for propagating particles to the next filtering distribution.

The algorithm consists of two steps:

Step 1. (Resample) Draw $\theta_t^{(i)} \sim Mult_N(w_t^{(1)}, \dots, w_t^{(N)})$ for $i = 1, \dots, N$

Step 2. (Propagate) Draw $\theta_{t+1}^{(i)} \sim p(\theta_{t+1} | \theta_t^{(i)}, y_{t+1})$ for $i = 1, \dots, N$.

To implement this algorithm, we need the predictive likelihood for the next observation, y_{t+1} , given the current state variable θ_t . It is defined by

$$p(y_{t+1}|\theta_t) = \int p(y_{t+1}|\theta_{t+1}) p(\theta_{t+1}|\theta_t) d\theta_{t+1}.$$

We also need the conditional posterior for the next states θ_{t+1} given (θ_t, y_{t+1}) . It is given by

$$p(\theta_{t+1}|\theta_t, y_{t+1}) \propto p(y_{t+1}|\theta_{t+1}) p(\theta_{t+1}|\theta_t).$$

This algorithm has several practical advantages. First, it does not suffer from the problem of particle degeneracy which plagues the standard sample-importance resample filtering algorithms. This effect is heightened when y_{t+1} is an outlier. Second, it can easily be extended to incorporate sequential parameter learning. It is common to also require learning about other unknown static parameters, denoted by ϕ . To do this, we assume that there exists a conditional sufficient statistic s_t for ϕ at time t , namely

$$p(\phi|\theta_{1:t}, y_{1:t}) = p(\phi|s_t)$$

where $s_t = s(\theta_{1:t}, y_{1:t})$. Moreover, we can propagate these sufficient statistics by the deterministic recursion $s_{t+1} = S(s_t, \theta_{t+1}, y_{t+1})$, given particles $(\theta_t, \phi, s_t)^{(i)}$, $i = 1, \dots, N$. First, we resample $(\theta_t, \phi, s_t)^{k(i)}$ with weights proportional to $p(y_{t+1}|(\theta_t, \phi)^{k(i)})$. Then we propagate to the next filtering distribution $p(\theta_{t+1}|y_{1:t+1})$ by drawing $\theta_{t+1}^{(i)}$ from $p(\theta_{t+1}|\theta_t^{k(i)}, \phi^{k(i)}, y_{t+1})$, $i = 1, \dots, N$. We next update the sufficient statistic for $i = 1, \dots, N$,

$$s_{t+1} = S(s_t^{k(i)}, \theta_{t+1}^{(i)}, y_{t+1}).$$

This represents a deterministic propagation. Parameter learning is completed by drawing $\phi^{(i)}$ using $p(\phi|s_{t+1}^{(i)})$ for $i = 1, \dots, N$. We now track the state, θ_t , and conditional sufficient statistics, s_t , which will be used to perform off-line learning for ϕ .

The algorithm now consists of four steps:

Step 1. (Resample) Draw Index $k_t(i) \sim \text{Mult}_N(w_t^{(1)}, \dots, w_t^{(N)})$ for $i = 1, \dots, N$

The weights are proportional to $p(y_{t+1}|(\theta_t, s_t)^{(i)})$

Step 2. (Propagate) Draw $\theta_{t+1}^{(i)} \sim p(\theta_{t+1}|(\theta_t, s_t)^{k(i)}, y_{t+1})$ for $i = 1, \dots, N$.

Step 3. (Update) Deterministic $s_{t+1}^{(i)} = S(s_t^{k(i)}, \theta_{t+1}^{(i)}, y_{t+1})$ for $i = 1, \dots, N$.

Step 4. (Learning) Offline $\phi^{(i)} \sim p(\phi|s_{t+1}^{(i)})$ for $i = 1, \dots, N$.

REFERENCES

- [1] Rasschaert, G., *Analysis of traffic data*. Master's thesis, Department of Electrical Energy, Systems and Automation, SYSTeMS, University of Ghent, Belgium, 2003.
- [2] Mihaylova, L., R. Boel, and A. Hegyi, Freeway traffic estimation within particle filtering framework. *Automatica*, Vol. 43, No. 2, 2007, pp. 290–300.

- [3] Tebaldi, C. and M. West, Bayesian inference on network traffic using link count data. *Journal of the American Statistical Association*, Vol. 93, No. 442, 1998, pp. 557–573.
- [4] Westgate, B. S., D. B. Woodard, D. S. Matteson, S. G. Henderson, et al., Travel time estimation for ambulances using Bayesian data augmentation. *The Annals of Applied Statistics*, Vol. 7, No. 2, 2013, pp. 1139–1161.
- [5] Anacleto, O., C. Queen, and C. J. Albers, Multivariate forecasting of road traffic flows in the presence of heteroscedasticity and measurement errors. *Journal of the Royal Statistical Society: Series C (Applied Statistics)*, Vol. 62, No. 2, 2013, pp. 251–270.
- [6] Kamijo, S., Y. Matsushita, K. Ikeuchi, and M. Sakauchi, Traffic monitoring and accident detection at intersections. *IEEE Transactions on Intelligent Transportation Systems*, Vol. 1, No. 2, 2000, pp. 108–118.
- [7] Gazis, D. C. and C. H. Knapp, On-line estimation of traffic densities from time-series of flow and speed data. *Transportation Science*, Vol. 5, No. 3, 1971, pp. 283–301.
- [8] Schreiter, T., C. van Hinsbergen, F. Zuurbier, H. Van Lint, and S. Hoogendoorn, Data-model synchronization in extended Kalman filters for accurate online traffic state estimation. In *2010 Proceedings of the Traffic Flow Theory Conference, Annecy, France, 2010*, Vol. 86.
- [9] Wang, Y. and M. Papageorgiou, Real-time freeway traffic state estimation based on extended Kalman filter: a general approach. *Transportation Research Part B: Methodological*, Vol. 39, No. 2, 2005, pp. 141 – 167.
- [10] Work, D. B., O.-P. Tossavainen, S. Blandin, A. M. Bayen, T. Iwuchukwu, and K. Tracton, An ensemble Kalman filtering approach to highway traffic estimation using GPS enabled mobile devices. In *Decision and Control, 2008. CDC 2008. 47th IEEE Conference on*, IEEE, 2008, pp. 5062–5068.
- [11] Blandin, S., A. Couque, A. Bayen, and D. Work, On sequential data assimilation for scalar macroscopic traffic flow models. *Physica D: Nonlinear Phenomena*, Vol. 241, No. 17, 2012, pp. 1421–1440.
- [12] Polson, N. and V. Sokolov, Bayesian Analysis of Traffic Flow on Interstate I-55: The LWR Model. *arXiv preprint arXiv:1409.6034*, 2014.
- [13] Lan, C.-J. and G. A. Davis, Real-time estimation of turning movement proportions from partial counts on urban networks. *Transportation Research Part C: Emerging Technologies*, Vol. 7, No. 5, 1999, pp. 305–327.
- [14] Ghods, A. H. and L. Fu, Real-time estimation of turning movement counts at signalized intersections using signal phase information. *Transportation Research Part C: Emerging Technologies*, Vol. 47, Part 2, 2014, pp. 128–138.
- [15] Kwong, K., R. Kavalier, R. Rajagopal, and P. Varaiya, Arterial travel time estimation based on vehicle re-identification using wireless magnetic sensors. *Transportation Research Part C: Emerging Technologies*, Vol. 17, No. 6, 2009, pp. 586–606.

- [16] Wu, C., J. Thai, S. Yadlowsky, A. Pozdnoukhov, and A. Bayen, Cellpath: Fusion of cellular and traffic sensor data for route flow estimation via convex optimization. *Transportation Research Part C: Emerging Technologies*, Vol. 59, 2015, pp. 111–128.
- [17] Rahmani, M., E. Jenelius, and H. N. Koutsopoulos, Non-parametric estimation of route travel time distributions from low-frequency floating car data. *Transportation Research Part C: Emerging Technologies*, Vol. 58, Part B, 2015, pp. 343–362.
- [18] Nantes, A., D. Ngoduy, A. Bhaskar, M. Miska, and E. Chung, Real-time traffic state estimation in urban corridors from heterogeneous data. *Transportation Research Part C: Emerging Technologies*, 2015.
- [19] Fowe, A. J. and Y. Chan, A microstate spatial-inference model for network-traffic estimation. *Transportation Research Part C: Emerging Technologies*, Vol. 36, 2013, pp. 245–260.
- [20] Dell’Orco, M., M. Marinelli, and M. A. Silgu, Bee Colony Optimization for innovative travel time estimation, based on a mesoscopic traffic assignment model. *Transportation Research Part C: Emerging Technologies*, 2015.
- [21] Coifman, B. and S. Kim, Speed estimation and length based vehicle classification from freeway single-loop detectors. *Transportation Research Part C: Emerging Technologies*, Vol. 17, No. 4, 2009, pp. 349–364.
- [22] Zheng, F. and H. Van Zuylen, Urban link travel time estimation based on sparse probe vehicle data. *Transportation Research Part C: Emerging Technologies*, Vol. 31, 2013, pp. 145–157.
- [23] Zhan, X., S. Hasan, S. V. Ukkusuri, and C. Kamga, Urban link travel time estimation using large-scale taxi data with partial information. *Transportation Research Part C: Emerging Technologies*, Vol. 33, 2013, pp. 37–49.
- [24] Seo, T. and T. Kusakabe, Probe vehicle-based traffic state estimation method with spacing information and conservation law. *Transportation Research Part C: Emerging Technologies*, Vol. 59, 2015, pp. 391–403.
- [25] Seo, T., T. Kusakabe, and Y. Asakura, Estimation of flow and density using probe vehicles with spacing measurement equipment. *Transportation Research Part C: Emerging Technologies*, Vol. 53, 2015, pp. 134–150.
- [26] Bachmann, C., B. Abdulhai, M. J. Roorda, and B. Moshiri, A comparative assessment of multi-sensor data fusion techniques for freeway traffic speed estimation using microsimulation modeling. *Transportation Research Part C: Emerging Technologies*, Vol. 26, 2013, pp. 33–48.
- [27] Vigos, G., M. Papageorgiou, and Y. Wang, Real-time estimation of vehicle-count within signalized links. *Transportation Research Part C: Emerging Technologies*, Vol. 16, No. 1, 2008, pp. 18–35.

- [28] Ban, X. J., P. Hao, and Z. Sun, Real time queue length estimation for signalized intersections using travel times from mobile sensors. *Transportation Research Part C: Emerging Technologies*, Vol. 19, No. 6, 2011, pp. 1133–1156.
- [29] Zhan, X., R. Li, and S. V. Ukkusuri, Lane-based real-time queue length estimation using license plate recognition data. *Transportation Research Part C: Emerging Technologies*, Vol. 57, 2015, pp. 85–102.
- [30] Lee, S., S. C. Wong, and Y. C. Li, Real-time estimation of lane-based queue lengths at isolated signalized junctions. *Transportation Research Part C: Emerging Technologies*, Vol. 56, 2015, pp. 1–17.
- [31] Sun, S., C. Zhang, and G. Yu, A bayesian network approach to traffic flow forecasting. *IEEE Transactions on Intelligent Transportation Systems*, Vol. 7, No. 1, 2006, pp. 124–132.
- [32] Horvitz, E. J., J. Apacible, R. Sarin, and L. Liao, Prediction, expectation, and surprise: Methods, designs, and study of a deployed traffic forecasting service. *arXiv preprint arXiv:1207.1352*, 2012.
- [33] Wu, C.-H., J.-M. Ho, and D. Lee, Travel-time prediction with support vector regression. *IEEE Transactions on Intelligent Transportation Systems*, Vol. 5, No. 4, 2004, pp. 276–281.
- [34] Quek, C., M. Pasquier, and B. Lim, POP-TRAFFIC: a novel fuzzy neural approach to road traffic analysis and prediction. *IEEE Transactions on Intelligent Transportation Systems*, Vol. 7, No. 2, 2006, pp. 133–146.
- [35] Rice, J. and E. van Zwet, A simple and effective method for predicting travel times on freeways. *IEEE Transactions on Intelligent Transportation Systems*, Vol. 5, No. 3, 2004, pp. 200–207.
- [36] Tan, M.-C., S. Wong, J.-M. Xu, Z.-R. Guan, and P. Zhang, An Aggregation Approach to Short-Term Traffic Flow Prediction. *IEEE Transactions on Intelligent Transportation Systems*, Vol. 10, No. 1, 2009, pp. 60–69.
- [37] Van Der Voort, M., M. Dougherty, and S. Watson, Combining Kohonen maps with ARIMA time series models to forecast traffic flow. *Transportation Research Part C: Emerging Technologies*, Vol. 4, No. 5, 1996, pp. 307–318.
- [38] Van Lint, J., Online Learning Solutions for Freeway Travel Time Prediction. *IEEE Transactions on Intelligent Transportation Systems*, Vol. 9, No. 1, 2008, pp. 38–47.
- [39] Ban, X. J., P. Hao, and Z. Sun, Real time queue length estimation for signalized intersections using travel times from mobile sensors. *Transportation Research Part C: Emerging Technologies*, Vol. 19, No. 6, 2011, pp. 1133–1156.
- [40] Ramezani, M. and N. Geroliminis, Queue profile estimation in congested urban networks with probe data. *Computer-Aided Civil and Infrastructure Engineering*, Vol. 30, No. 6, 2015, pp. 414–432.

- [41] Cheng, Y., X. Qin, J. Jin, and B. Ran, An exploratory shockwave approach to estimating queue length using probe trajectories. *Journal of Intelligent Transportation Systems*, Vol. 16, No. 1, 2012, pp. 12–23.
- [42] Hofleitner, A., R. Herring, P. Abbeel, and A. Bayen, Learning the dynamics of arterial traffic from probe data using a dynamic Bayesian network. *Intelligent Transportation Systems, IEEE Transactions on*, Vol. 13, No. 4, 2012, pp. 1679–1693.
- [43] Van Lint, J. and S. P. Hoogendoorn, A robust and efficient method for fusing heterogeneous data from traffic sensors on freeways. *Computer-Aided Civil and Infrastructure Engineering*, Vol. 25, No. 8, 2010, pp. 596–612.
- [44] West, M. and J. Harrison, *Bayesian Forecasting and Dynamic Models (Springer Series in Statistics)*. Springer-Verlag, 1997.
- [45] Carlin, B. P., N. G. Polson, and D. S. Stoffer, A Monte Carlo approach to nonnormal and nonlinear state-space modeling. *Journal of the American Statistical Association*, Vol. 87, No. 418, 1992, pp. 493–500.
- [46] Smith, B. L., B. M. Williams, and R. Keith Oswald, Comparison of parametric and non-parametric models for traffic flow forecasting. *Transportation Research Part C: Emerging Technologies*, Vol. 10, No. 4, 2002, pp. 303–321.
- [47] Chiou, Y.-C., L. W. Lan, and C.-M. Tseng, A novel method to predict traffic features based on rolling self-structured traffic patterns. *Journal of Intelligent Transportation Systems*, Vol. 18, No. 4, 2014, pp. 352–366.
- [48] Lighthill, M. J. and G. B. Whitham, On kinematic waves. II. A theory of traffic flow on long crowded roads. *Proceedings of the Royal Society of London. Series A. Mathematical and Physical Sciences*, Vol. 229, No. 1178, 1955, pp. 317–345.
- [49] Richards, P. I., Shock waves on the highway. *Operations research*, Vol. 4, No. 1, 1956, pp. 42–51.
- [50] Carvalho, C. M., M. S. Johannes, H. F. Lopes, and N. G. Polson, Particle learning and smoothing. *Statistical Science*, Vol. 25, No. 1, 2010, pp. 88–106.
- [51] Gordon, N. J., D. J. Salmond, and A. F. Smith, Novel approach to nonlinear/non-Gaussian Bayesian state estimation. In *IEE Proceedings F (Radar and Signal Processing)*, IET, 1993, Vol. 140 (2), pp. 107–113.
- [52] Carpenter, J., P. Clifford, and P. Fearnhead, Improved particle filter for nonlinear problems. *IEE Proceedings-Radar, Sonar and Navigation*, Vol. 146, No. 1, 1999, pp. 2–7.
- [53] Pitt, M. K. and N. Shephard, Filtering via simulation: Auxiliary particle filters. *Journal of the American statistical association*, Vol. 94, No. 446, 1999, pp. 590–599.
- [54] Storvik, G., Particle filters for state-space models with the presence of unknown static parameters. *Signal Processing, IEEE Transactions on*, Vol. 50, No. 2, 2002, pp. 281–289.